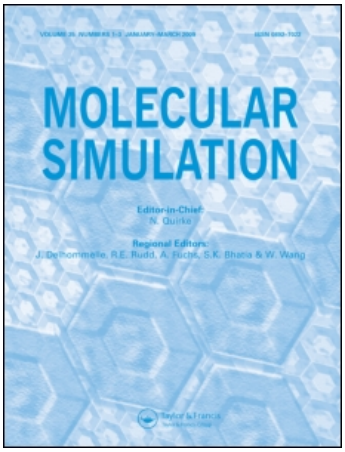

Molecular Simulation
Publication details, including instructions for authors and subscription information:
http://www.informaworld.com/smpp/title~content=t713644482

Molecular Dynamics Studies of the Dielectric Constant of Dipolar Fluids: Dependence on Molecular Shape

P. A. Wielopolski[ab]; E. R. Smith[ac]
[a] Mathematics Department, University of Melbourne, Victoria, Australia [b] Institute of Physical Chemistry, Polish Academy of Sciences, Warsaw, Poland [c] Mathematics Department, LaTrobe University, Victoria, Australia

To cite this Article Wielopolski, P. A. and Smith, E. R.(1988) 'Molecular Dynamics Studies of the Dielectric Constant of Dipolar Fluids: Dependence on Molecular Shape', Molecular Simulation, 1: 3, 157 — 167
To link to this Article: DOI: 10.1080/08927028808080939
URL: http://dx.doi.org/10.1080/08927028808080939

Molecular Simulation, 1988, Vol. 1, pp. 157–167

MOLECULAR DYNAMICS STUDIES OF THE DIELECTRIC CONSTANT OF DIPOLAR FLUIDS: DEPENDENCE ON MOLECULAR SHAPE

P.A. WIELOPOLSKI* and E.R. SMITH‡

Mathematics Department, University of Melbourne, Parkville, Victoria 3052, Australia

(*Received April 1987; in final form July 1987*)

We report simulation calculations of the static dielectric constant and other distribution functions for a fluid sample of 125 two-centre Lennard-Jones molecules. The molecular dipole moment was due to equal and opposite partial point charges on the Lennard-Jones centres. The system was varied by keeping density, temperature, molecular dipole moments, centre–centre distance and molecule volume fixed and varying the ratio R of the two Lennard-Jones σ-parameters, while keeping the thermodynamic state roughly constant by suitable adjustment of the Lennard-Jones ε-parameters. The dielectric constant showed a pronounced minimum at $R \simeq 2/3$. The dependence of the dielectric constant on R is discussed in terms of the changes observed in the short-range structure of the fluid as R changed.

KEY WORDS: Molecular dynamics, dielectric constants, dipolar fluids.

1.1 INTRODUCTION

Until very recently, simulation studies of the dielectric constant of polar fluids have concentrated on systems of molecules of very simple structure, such as the system of hard spheres with embedded point dipoles or the Stockmayer fluid. Dielectric properties of such systems can now be calculated by simulation. Later, attention turned to more complex molecules so that the influence of molecular shape and of non-central force laws could be investigated. The rather limited results available at present show that replacing a spherical core with a dumb-bell shaped core, or replacing a point dipole in a hard sphere with a pair of separated charges within the hard sphere, reduces the dielectric constant.

This dielectric constant reduction was first demonstrated by Morriss and Cummings [1] who studied a point charge model of chloromethane. Morriss [2] studied symmetric polar hard dumb-bells and showed that the dielectric constant decreased monotonically with increase in elongation of the dumb-bell. DeLeeuw and Quirke [3] found similar behaviour in symmetric two-centre Lennard-Jones molecules. As the molecules are elongated, packing effects increase the probability of antiparallel alignment of nearest neighbour dipoles compared with the probability of antiparallel alignment in a fluid of spherical dipolar molecules. This increased antiparallel alignment decreases the mean square dipole moment fluctuations in the

*Present address: Research School of Chemistry, ANU, PO Box 4, ACT 2601, Australia. Permanent address: Institute of Physical Chemistry, Polish Academy of Sciences, Warsaw, Poland.
‡Present address: Mathematics Department, LaTrobe University, Bundoora, Victoria 3083, Australia.

system and so decreases the dielectric constant. Isbister and Morriss [4] have studied a system of hard spheres carrying separated charges within them to give a finite dipole moment. As the charge separation increases (with the dipole moment kept fixed), the dielectric constant increases, thus illustrating the importance of steric effects in the dumb-bell case. Wielopolski and Smith [5] studied two models of ethylene oxide (C_2H_4O) molecules. The models differed in the Lennard-Jones parameters assigned to interactions between the three interaction sites on the model molecules. The model for which the "Star of David" configuration (an antiparallel dipole configuration) had lower energy had a lower dielectric constant, thus reinforcing this view of the importance of sterically induced antiparallel alignment in determining dielectric constants. Hesse-Bezot *et al.* [6] have reported dielectric constants for Lennard-Jones spheres with off-centre point dipoles. They report a dramatic decrease in dielectric constant as the dipoles become more off-centred.

In this paper we consider asymmetric two-centre Lennard-Jones molecules of varying shapes and examine the effects of shape variation on dielectric constant. The model molecules are composed of two Lennard-Jones centres kept a fixed distance apart, each bearing constant charges so that the molecules are electrostatically neutral and have a fixed dipole moment. The shape of the molecules is varied by changing the Lennard-Jones diameters of the two centres. Thus, if the two centres of molecule j are at $\mathbf{r}_{j,1}$ and $\mathbf{r}_{j,2}$, carrying charges q_1 and $q_2 = -q_1$, the dipole moment of molecule j is $\boldsymbol{\mu}_j = q_1(\mathbf{r}_{j,1} - \mathbf{r}_{j,2})$ and the site–site interactions are

$$\phi_{\alpha,\beta}(\mathbf{r}_{j,\alpha}, \mathbf{r}_{k,\beta}) = 4\varepsilon_{\alpha\beta}[(|\mathbf{r}_{j,\alpha} - \mathbf{r}_{k,\beta}|/\sigma_{\alpha,\beta})^{-12} - (|\mathbf{r}_{j,\alpha} - \mathbf{r}_{k,\beta}|/\sigma_{\alpha\beta})^{-6}]. \quad (1)$$

The parameters $\varepsilon_{\alpha\beta}$, $\sigma_{\alpha\beta}$ obey the usual Lorentz–Berthelot combining rules,

$$\sigma_{12} = \tfrac{1}{2}(\sigma_{1,1} + \sigma_{2,2}), \; \varepsilon_{12} = (\varepsilon_{1,1}\varepsilon_{2,2})^{1/2}.$$

The magnitude $l = |\mathbf{r}_{j,1} - \mathbf{r}_{j,2}|$ is kept fixed and so is $|\boldsymbol{\mu}_j| = lq_1$. A "hard-core" molecular volume may be defined by calculating the excluded volume of a dumb-bell of two spheres with centre-to-centre distance l and sphere radii $\sigma_{1,1}$ and $\sigma_{2,2}$. This volume is kept fixed so that $\sigma_{2,2}$ is a function of $\sigma_{1,1}$ as the shape changes. To attempt to keep an equivalent thermodynamic state as the shape changes, not only is this hard-core volume kept constant, but the energy parameters are rescaled to keep the molecular second virial coefficient of the molecules fixed and equal to that for the free atoms. This form of shape variation thus provides a molecular model whose dielectric properties may be expected to be partly those of an elongating molecule and partly those of a spherical model with off-centre dipole moments. Molecular dynamics simulations were performed for s values of the diameter ratio $R = \sigma_{2,2}/\sigma_{1,1}$ in the range $1/3 \leqslant R \leqslant 1$.

2 DETAILS OF MOLECULAR MODEL AND SIMULATIONS

The model molecules consist of two rigidly bound Lennard-Jones atoms carrying a partial charge $\pm q$. The centre-to-centre distance is 1.784 Å, corresponding to CH_3Cl and the magnitude of the partial charges gives a molecular dipole moment of 1.87 D. The dipole magnitude and centre-to-centre distances are kept constant in all the simulations reported.

The two centres of molecule j are at $\mathbf{r}_{j,1}$ (with charge $+q$) and $\mathbf{r}_{j,2}$ (with charge

$-q$) for each j in $1 \leqslant j \leqslant N$. The Hamiltonian for the N-molecule system may be written

$$\mathscr{H} = \mathscr{H}_{L-J} + \mathscr{H}_E(\varepsilon') + T. \tag{2}$$

Here, T is the kinetic energy of the molecules and

$$\mathscr{H}_{L-J} = \frac{1}{2} \sum_{\substack{j=1 \\ j \neq k}}^{N} \sum_{k=1}^{N} \sum_{\alpha=1}^{2} \sum_{\beta=1}^{2} \phi_{L-J}(|\bar{\mathbf{r}}_{jk}^{\alpha\beta}|; \alpha, \beta) \tag{3}$$

with $\bar{\mathbf{r}}_{jk}^{\alpha\beta}$ defined as the minimum image convention replica of $\mathbf{r}_{jk}^{\alpha\beta} = \mathbf{r}_{j,a} - \mathbf{r}_{k,\beta}$, and

$$\phi_{L-J}(r; \alpha, \beta) = 4\varepsilon_{\alpha\beta}[(r/\sigma_{\alpha,\beta})^{-12} - (r/\sigma_{\alpha,\beta})^{-6}]. \tag{4}$$

The electrostatic part $\mathscr{H}_E(\varepsilon')$ of the Hamiltonian is calculated according to the periodic boundary condition technique developed by DeLeeuw, Perram and Smith [7] and adapted to the needs of this work by us in an earlier paper [5]. The dielectric constant ε of the system modelled in this way is given by the relation

$$\frac{(\varepsilon - 1)(2\varepsilon' + 1)}{3(\varepsilon + 2\varepsilon')} = yg(\varepsilon') \tag{5}$$

where ε' is an external medium dielectric constant. The g-factor is given by

$$g(\varepsilon') = [\langle \mathbf{M}^2 \rangle_{\varepsilon'} - \langle \mathbf{M} \rangle_{\varepsilon'}^2]/N\mu^2 \tag{6}$$

with $\langle\ \rangle_{\varepsilon'}$ being a simulation average calculated with the Hamiltonian (2), μ being the fixed dipole magnitude and $\mathbf{M}$ being the net dipole moment of a configuration, namely

$$\mathbf{M} = \sum_{j=1}^{N} \sum_{\alpha=1}^{2} q_\alpha \mathbf{r}_{j,\alpha}. \tag{7}$$

In Equation (5), the dimensionless parameter y is given as

$$y = 4\pi\rho\mu^2/9kT \tag{8}$$

In this paper we use the $\varepsilon' \to \infty$ limit which gives

$$\varepsilon = 1 + 3yg(\infty). \tag{9}$$

Earlier papers [1, 8] have observed that, in this limit, estimates of the dielectric constant derived from mean square dipole moment fluctuation formulae like (5) converge most quickly to their final value.

The molecular dynamics simulations used the Verlet algorithms [9] with independent Cartesian coordinates for each Lennard-Jones centre. The molecular bond length ws constrained with a SHAKE-type algorithm [10]. This was implemented as follows: The particles of each molecule were first allowed to move in each time step without constraint. They were then moved back onto the constraint surface in phase space by forces along the bond at the start of the time step. This provided the end state of each time step. The particular move used back onto the constraint surface was generated by the solution of quadratic equations. These were solved by a Newton Raphson iteration. The starting solution for the iteration was taken as the solution for each bond considered independently. These starting solutions were generated by the formula for the solutions of a quadratic equation, care being taken to use that solution corresponding to a small shift. The simulation sample consisted of 125 molecules in a cubic box of length $L = 22.6373$ Å, which corresponds to the number

Table 1 Lennard-Jones potential parameters used for the five molecular dynamics simulations.

Run	$R = \sigma_{22}/\sigma_{11}$	$\sigma_{11}(\AA)$	$\frac{\varepsilon_{11}}{k}[K]$	$\sigma_{22}(\AA)$	$\frac{\varepsilon_{22}}{k}[K]$
A1	1	3.5	114.13	3.5	114.13
A2	5/6	3.77282	106.2644	3.14402	128.0152
A3	2/3	3.98218	101.641	2.65479	159.4837
A4	1/2	4.10836	99.5893	2.05418	239.5069
A5	1/3	4.1632	98.5275	1.387733	467.0716

density of liquid CH_3Cl at 253 K. The time step used was 0.009 ps. The total energy was checked every 400 time steps and deviated from the mean value in each averaging run of 27 000 time steps by less than one part in 10^5. The charges used throughout were

$$q_1 = 0.218227\,Q,\ q_2 = -0.218227\,Q$$

with $Q = 1.6022 \times 10^{-19}$C. The bond length was $l = 1.787$ Å. The sets of Lennard-Jones parameters used are listed for the runs A1 to A5 in Table 1.

As noted in the introduction, these parameter choices preserve the "hard-core" volume of the molecule and the second virial coefficients of the free atoms, namely

$$\sum_{\alpha=1}^{2}\sum_{\beta=1}^{2}\int d^3\mathbf{r}\,[\exp\,[-\rho\phi(|r|;\alpha,\beta)] - 1], \tag{10}$$

at 255 K is kept constant.

3 RESULTS AND DISCUSSION

Thermodynamic Properties

Throughout the simulation the total energy, potential energy and pressure were monitored. Every 400 time steps the ratio of rotational and translational kinetic

Table 2 Thermodynamic data for the five model systems. The asterisk indicates that these items have had a long-range L–J potential correction due to the potential outside the minimum image cube added.

Thermodynamic quantity	*A1*	*A2*	*A3*	*A4*	*A5*	*Max % error*
Temperature $T(K)$	255.902	251.12	257.643	261.274	255.99	1.0
Total energy $\mathscr{H}/NkT$	−3.4922	−3.5496	−3.166	−2.9035	−3.039	0.05
Total potential energy $\frac{[\mathscr{H}_{L-J} + \mathscr{H}(\varepsilon')]}{NkT}$	−6.114	−6.173	−5.782	−5.512	−5.643	0.5
L–J contribution* $\mathscr{H}_{L-J}/NkT$	−4.966	−4.973	−4.551	−4.134	−3.944	0.5
Charge–charge contribution $\mathscr{H}(\varepsilon')/NkT$	−1.148	−1.2	−1.231	−1.378	−1.699	1.0
PV/NkT*	−0.117	−0.141	0.107	0.232	0.039	?
T_{Rot}/T_{trans}	0.67	0.671	0.699	0.676	0.674	3

energies was sampled and remained close to 0.666, indicating that equilibrium between rotational and translational degrees of freedom was achieved. The thermodynamic results are given in Table 2.

All runs were preceded by 25 000 time step equilibrium runs. Errors were estimated by taking the range of subaverages of four blocks of 7000, 7000, 7000 and 6000 time steps. The results in Table 2 indicate that, despite the differing L–J parameters, all the systems investigated were at roughly the same thermodynamic state. Thus it is possible to make meaningful comparisons between dielectric properties and structural data for the different systems.

Dielectric Constant and Angular Correlation Functions

It is useful to define an "equivalent Stockmayer system" of Lennard-Jones spheres with $\sigma = 2.0879$ Å, reduced dipole moment $\mu^{*2} = \mu^2/8\sigma^3 kT = 1.364$, reduced density $\rho^* = 8(N/V)\sigma^3 = 0.7846$, and $\varepsilon/k = 189$ K. This Stockmayer system has the same dipole magnitude, particle volume and second virial coefficient as our molecules. Linear interpolation of the Pollock and Alder results [11] gives $\varepsilon \simeq 15$ for this equivalent Stockmayer system.

Figure 1 presents a plot of the dielectric constant as a function of the diameter ratio $R = \sigma_{22}/\sigma_{11}$. The cases $R = 1$ and $R = 0.1455$ correspond to completely symmetric dumb-bells and to spherical molecules with $\sigma = 2.0879$ Å, respectively. The spherical molecule case has two L–J centres and an off-centre dipole moment at 0.105σ from the centre of the sphere.

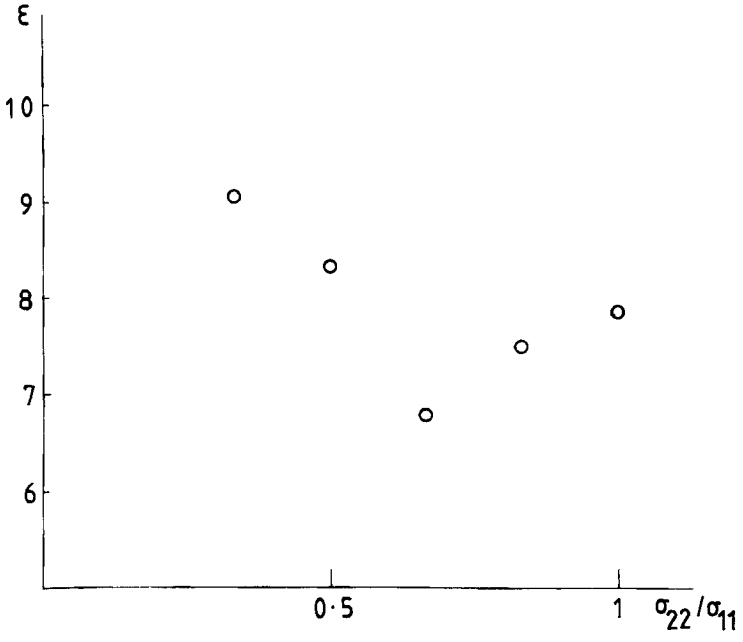

Figure 1 Plot of dielectric constant as a function of R = σ_{22}/σ_{11}.

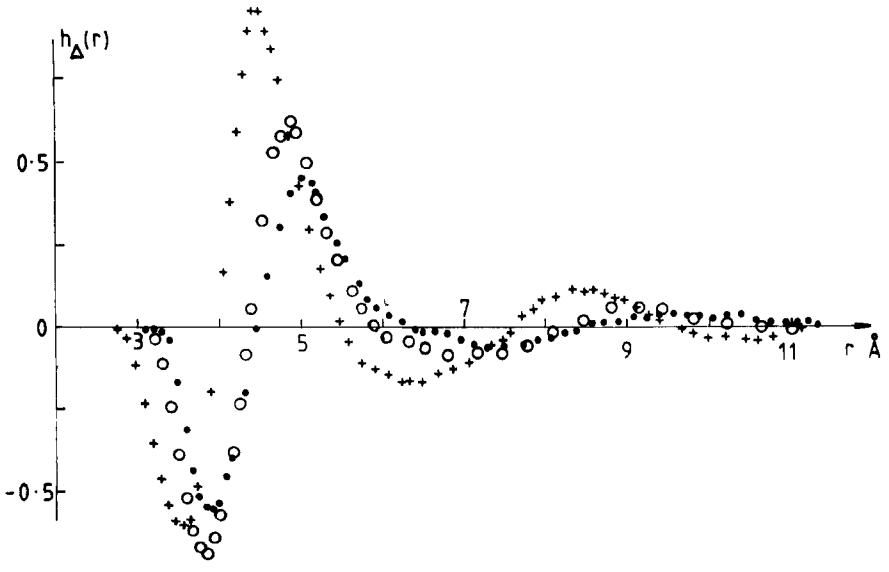

Figure 2 Graph of $h_\Delta(r)$; A1: ●; A3: ○; A5: +.

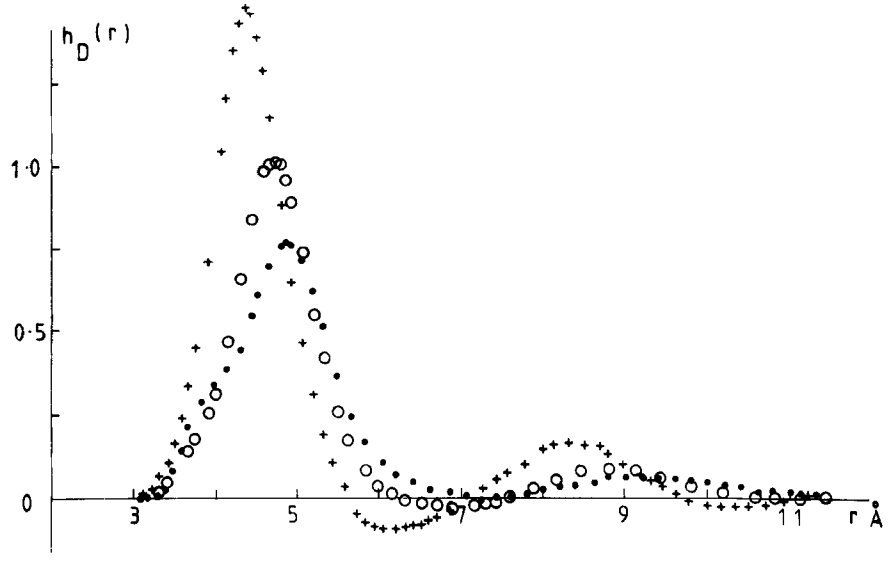

Figure 3 Graph of $h_D(r)$; A1: ●; A3: ○; A5: +.

The estimates of ε were found by plotting the average estimate of ε against simulation time. The circles in Figure 1 represent $\frac{1}{2}$ the range of the variation in this plot over the last 7000 time steps of each run.

Table 3 Positions of maxima and minima of angular correlation function $h_\Delta(r)$.

System	*1st min*		*1st max*		*2nd min*		*2nd max*	
	r(Å)	*Height*	*r(Å)*	*Height*	*r(Å)*	*Height*	*r(Å)*	*Height*
A1	4.00	−0.53	4.99	0.455	7.42	−0.057	9.6	0.045
A2	3.84	−0.578	4.99	0.495	7.06	−0.066	9.43	0.045
A3	3.83	−0.683	4.86	0.625	7.02	−0.077	9.05	0.055
A4	3.66	−0.666	4.66	0.804	6.74	−0.116	8.73	0.1
A5	3.58	−0.595	4.52	0.955	6.3	−0.168	8.4	0.12

For symmetric dumb-bells (with $l^* = l/\sigma = 0.5$) the dielectric constant is about 50% of that for the equivalent Stockmayer system. This result compares well with those reported in [2] and [3]. As r decreases, the dielectric constant reaches a minimum at $R \simeq 2/3$, suggesting that the antiparallel aligned configuration of nearest neighbour dipoles is most stable for this particular molecular geometry. Figures 2 and 3 show plots of the angular correlation functions $h_\Delta(r)$ and $h_D(r)$, and the positions of some of the features of these functions are tabulated in Tables 3 and 4. These data support our conclusions about the way in which the importance of the nearest neighbour antiparallel alignment is affected by molecular geometry.

These site–site distribution functions indicate a significant change in the structure of the liquid as R decreases. As R decreases, the function $g_{++}(r)$ becomes closer to that for a monatomic liquid. The function $g_{--}(r)$ shows that the smaller spheres of the dumb-bells are effectively uncorrelated beyond the first shell or peak in the distribution functions. A much more interesting charge is shown by $g_{+-}(r)$. As R decreased beyond 2/3, $g_{+-}(r)$ begins to develop a second maximum fairly close to the first one. When compared with the graphs of $h_\Delta(r)$ and $h_D(r)$, the first maximum of $g_{+-}(r)$ is seen to be due to closest approach of antiparallel aligned molecules, while this second maximum corresponds to antiparallel alignment; in the head-to-head configuration, however, the negative charges on the smaller spheres are pushed together by packing effects. Further, the structure suggests that the first maximum in the $g_{--}(r)$ function corresponds to both head-to-head and head-to-tail configurations of the dipoles.

The case $R = 2/3$ has the deepest first minimum in $h_\Delta(r)$, showing that nearest neighbour pairs are most strongly aligned antiparallel for this value of R. As R decreases further, the dielectric constant rises again and by an approximate extrapolation reaches 9.5 at $R = 0.1455$. This value is about 65% of that for the equivalent Stockmayer system, and thus demonstrates again that decentralizing the dipole does indeed decrease the dielectric constant, as was shown in [6]. However, our results show that non-spherical molecular geometry can cause a much larger decrease in dielectric

Table 4 Positions of maxima and minima of the angular correlation function $h_D(r)$.

System	*1st max*		*1st min*		*2nd max*		*2nd min*	
	r(Å)	*Height*	*r(Å)*	*Height*	*r(Å)*	*Height*	*r(Å)*	*Height*
A1	4.86	0.763	7.15	0.0	8.8	0.061	–	–
A2	4.86	0.842	7.15	−0.008	9.1	0.077	–	–
A3	4.73	1.02	6.85	−0.028	8.8	0.094	–	–
A4	4.59	1.24	6.45	−0.059	8.62	0.138	10.7	−0.0135
A5	4.38	1.48	6.1	−0.094	8.39	−0.174	10.46	−0.0264

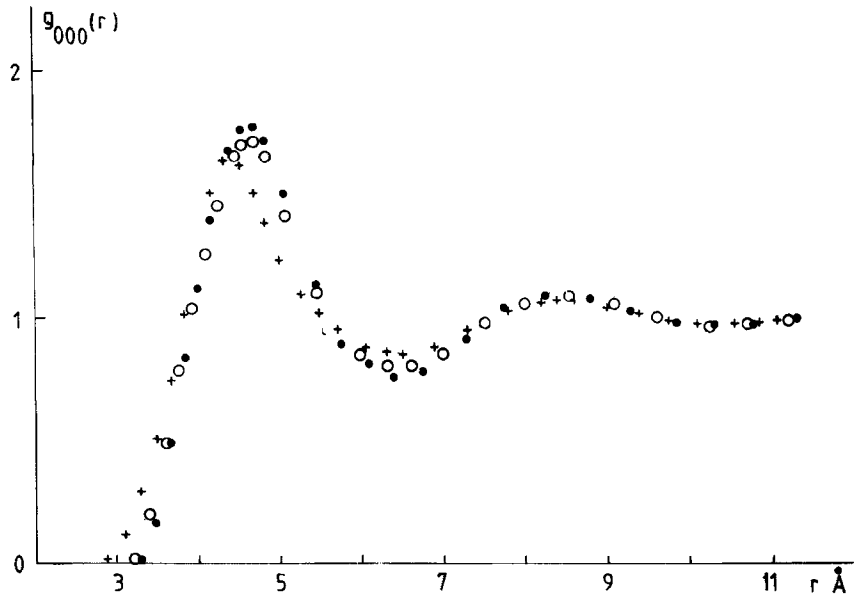

Figure 4 Plot of $g_{000}(r)$: Al: ●; A3: ○; A5: +.

Table 5 Positions of maxima and minima of radial distribution function $g_{000}(r)$.

System	*1st max*		*1st min*		*2nd max*		*2nd min*	
	r(Å)	*Height*	*r(Å)*	*Height*	*r(Å)*	*Height*	*r(Å)*	*Height*
A1	4.6	1.78	6.37	0.763	8.62	1.1	10.5	0.965
A2	4.6	1.77	6.35	0.772	8.43	1.095	10.46	0.957
A3	4.6	1.71	6.5	0.803	8.47	1.097	10.32	0.965
A4	4.6	1.68	6.4	0.835	8.54	1.084	10.47	0.97
A5	4.4	1.65	6.45	0.835	8.5	1.071	10.39	0.976

constant than can setting the dipole off centre, and that this decrease is due to a change in short-range structure due to packing effects, which in turn decrease the mean square dipole moment fluctuations.

Short-range Structure

Figure 4 and Table 5 describes the centre of mass–centre of mass radial distribution functions $g_{000}(r)$.

Apart from model A5, the $g_{000}(r)$ curves are very similar for all the model systems; in the A5 case, the main change is an approximately 4% decrease in the distance to the first maximum. This is in spite of a large potential variation between the models, supporting our contention that the models are all at equivalent thermodynamic states.

Table 6 and Figures 5, 6 and 7 describe the site–site correlation functions $g_{\alpha,\beta}(r)$, α, $\beta = 1, 2$.

Table 6 Positions of maxima and minima of site–site distribution functions $g_{\alpha\beta}(r)$.

System$_{\alpha\beta}$	*1st max*		*1st min*		*2nd max*		*2nd min*	
	r(Å)	*Height*	*r(Å)*	*Height*	*r(Å)*	*Height*	*r(Å)*	*Height*
A1:	σ_{11} = 3.5 Å		σ_{22} = 3.5 Å		l = 1.787			
	g_{++} 4.16–5.18	1.365	6.45	0.844	8.35	1.05	10.55	0.98
	g_{--} 4.16–5.18	1.365	6.45	0.844	8.35	1.05	10.55	0.98
	g_{+-} 3.75	1.63	6.45	0.9	8.35	1.06	10.55	0.98
A2:	σ_{11} = 3.773		σ_{22} = 3.144					
	g_{++} 4.38	1.61	6.5	0.795	8.6	1.08	10.45	0.97
	g_{--} 5.06	1.34	6.35	0.88	8.6	1.036	Not seen	
	g_{+-} 3.75	1.625	6.45	0.92	8.13	1.055	10.13	0.982
A3:	σ_{11} = 3.982		σ_{22} = 2.65					
	g_{++} 4.45	1.86	6.4	0.77	8.58	1.12	10.45	0.95
	g_{--} 4.95	1.3	6.3	0.93	8.5	1.02	Not seen	
	g_{+-} 3.66	1.53	5.06	0.96	5.65	1.0	6.64	0.948
A4:	σ_{11} = 4.10		σ_{22} = 2.05					
	g_{++} 4.45	2.1	6.4	0.741	8.58	1.15	10.45	0.938
	g_{--} 4.8	1.3	6.3	0.951	Not seen		Not seen	
	g_{+-} 3.48	1.39	4.66	0.924	5.77	1.05	6.74	0.976
A5:	σ_{11} = 4.16		σ_{22} = 1.38					
	g_{++} 4.52	2.3	6.4	0.735	8.5	1.16	10.3	0.929
	g_{--} 4.55	1.3	6.3	0.955	Not seen		Not seen	
	g_{+-} 3.2	1.3	4.25	0.863	5.82	1.1	Not seen	

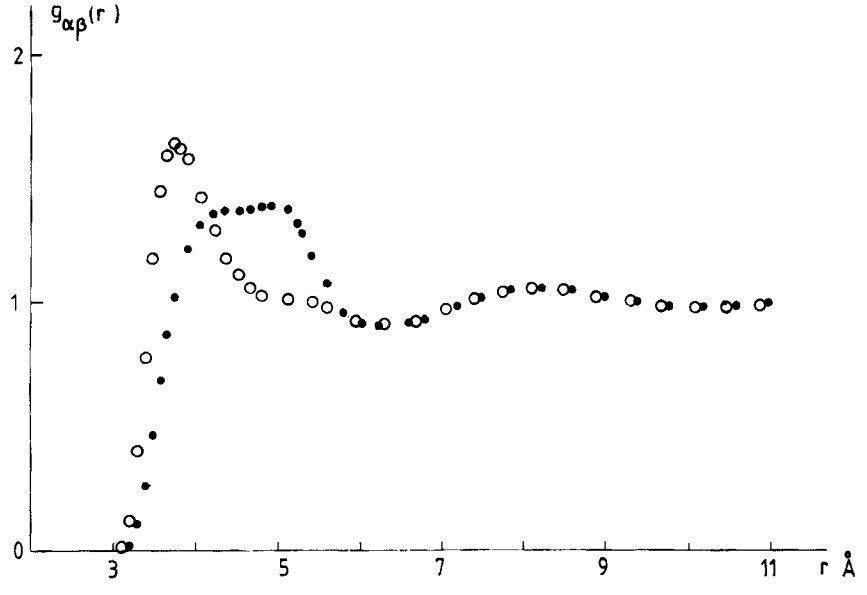

Figure 5 Plot of $g_{\alpha\beta}(r)$ for state A1; g_{++}: ●; g_{+-}: ○.

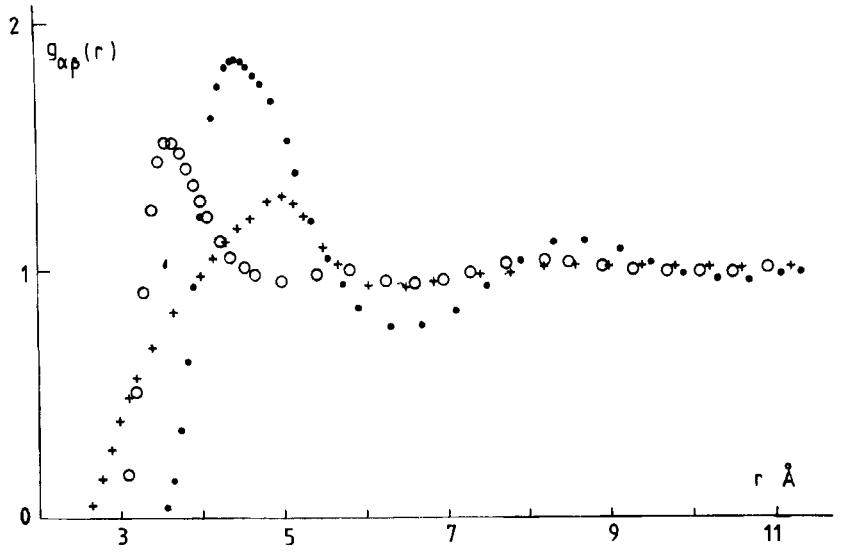

Figure 6 Plot of $g_{\alpha\beta}(r)$ for A3; $g_{++}(r)$: ●; $g_{+-}(r)$: ○; $g_{--}(r)$: +.

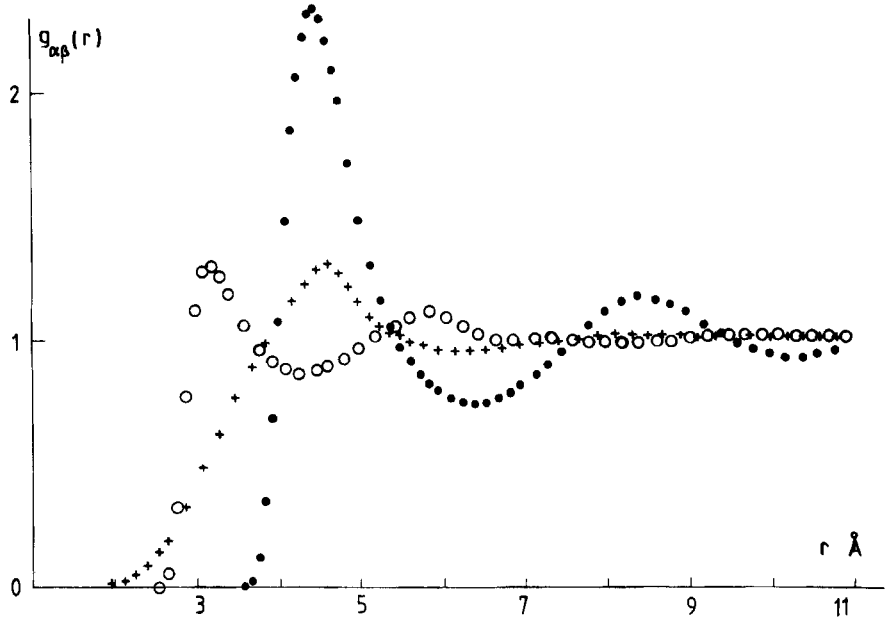

Figure 7 Plot of $g_{\alpha\beta}(r)$ for A5; $g_{++}(r)$: ●; $g_{+-}(r)$: ○; $g_{--}(r)$: +.

References

[1] G.P. Morriss and P.T. Cummings, "The dielectric constant of polar hard dumb-bells. A point charge model for chloromethane", *Molec. Phys.*, **45**, 1099 (1982).

[2] G.P. Morriss, "The dielectric constant of polar hard dumb-bells. Dependence on molecular shape", *Molec. Phys.*, **47**, 833 (1982).

[3] S.W. DeLeeuw and N. Quirke, "Dielectric behaviour and multibody orientational correlations of dipolar molecular liquids", *J. Chem. Phys.*, **81**, 880 (1984).

[4] G.P. Morriss and D.J. Isbister, "The phase behaviour of interaction site fluids", *Molec. Phys.*, **52**, 57 (1984).

[5] P.A. Wielopolski and E.R. Smith, "Molecular dynamics studies of dielectric behaviour and orientational correlations of liquid ethyleneoxide (oxirane)", *Molec. Phys.*, **54**, 467 (1985)

[6] C. Hesse-Bezot, G. Bossis and C. Brot, "New molecular dynamics simulation of a 3d fluid of Stockmayer and modified Stockmayer particles", *J. Chem. Phys.*, **80**, 3399 (1984).

[7] S.W. DeLeeuw, J.W. Perram and E.R. Smith: "Simulation of electrostatic systems in periodic boundary conditions. I. Lattice sums and dielectric constants", *Proc. Roy. Soc. (Lond.)*, **A373**, 27 (1980); and "Simulation of electrostatic systems in periodic boundary conditions. II. Equivalence of boundary conditions", ibid., **A373**, 57 (1980).

[8] S.W. DeLeeuw, J.W. Perram and E.R. Smith, "Simulation of electrostatic systems in periodic boundary conditions. III. Further theory and applications", *Proc. Roy. Soc. (Lond.)*, **A388**, 177 (1983).

[9] L. Verlet, "Computer 'experiments' on classical fluids. I. Thermodynamical properties of Lennard-Jones molecules", *Phys. Rev.*, **159**, 98 (1967).

[10] H.J.C. Berendsen and W.F. van Gunsteren, "Molecular dynamics with constraints", in *The Physics of Superionic Conductor and Electrode Materials*, J.W. Perram, ed., Plenum, New York, 1983, ch. 12.

[11] E.L. Pollock and B.J. Adler, "Static dielectric properties of Stockmayer fluids", *Physica A*, **102A**, 1 (1980).